

# An Unsymmetric Trinuclear Chromium(III) Oxo Carboxylate Assembly: Structure and Characterization of $\text{Cr}_3\text{O}(\text{O}_2\text{CPh})_4(\text{8-hqn})_3 \cdot 1.25\text{CH}_2\text{Cl}_2$

Maysa K. Nagi,<sup>1</sup> Anthony Harton,<sup>1</sup> Scott Donald,<sup>1</sup> Young-Sook Lee,<sup>2</sup> Michal Sabat,<sup>\*,3</sup> Charles J. O'Connor,<sup>\*,2</sup> and John B. Vincent<sup>\*,1</sup>

Departments of Chemistry, University of Alabama, Tuscaloosa, Alabama 35487-0336, University of Virginia, Charlottesville, Virginia 22903, and University of New Orleans, New Orleans, Louisiana 70148

Received December 27, 1994<sup>®</sup>

The structural and spectroscopic properties of a series of unsymmetric trinuclear chromium–oxo complexes are reported. One example,  $\text{Cr}_3\text{O}(\text{O}_2\text{CPh})_4(\text{8-hqn})_3 \cdot 1.25\text{CH}_2\text{Cl}_2$  crystallizes in the triclinic space group  $P\bar{1}$  (No. 2) with  $a = 11.901(2)$  Å,  $b = 19.410(4)$  Å,  $c = 11.701(1)$  Å,  $\alpha = 96.58(1)^\circ$ ,  $\beta = 95.66(1)^\circ$ ,  $\gamma = 101.21(1)^\circ$ ,  $V = 2614(1)$  Å<sup>3</sup>, and  $Z = 2$ . The structure was refined with 4869 reflections having  $I > 3.00\sigma(I)$  giving final values of 0.057 and 0.069 for  $R$  and  $R_w$ , respectively. The  $[\text{Cr}_3\text{O}]^{7+}$  core of the complex is distinctly unsymmetric with Cr–Cr separations of 2.909(1), 3.235(1), and 3.466(2) Å and Cr–O–Cr angles of 94.4(2), 118.1(2), and 130.2(2)°. The magnetic susceptibility of complex 1 was measured in the range 8–300 K. The effective moment per molecule decreases from 6.36  $\mu_B$  at 300 K to 4.0  $\mu_B$  at 15 K, which is appropriate for a system with a spin  $3/2$  ground state. Below 15 K, the magnetic moment varies little with temperature. The significance of these results in terms of the molecule's structure is discussed. Results of <sup>1</sup>H and <sup>2</sup>H NMR, EPR, and mass spectral studies are presented.

## Introduction

Trinuclear oxo-centered metal carboxylate assemblies of the general composition  $[\text{M}_3\text{O}(\text{O}_2\text{CR})_6\text{L}_3]^{n+}$  have been of intense interest for several decades as they have served as important models to test theories of magnetic coupling between metal ions in multinuclear systems.<sup>4</sup> These "basic metal carboxylates" where  $\text{M} = \text{Cr}^{\text{III}}$  display weak antiferromagnetic coupling. Attempts to model the variable-temperature bulk magnetic susceptibility of the materials to quantitate the coupling constants via a symmetric Heisenberg approach have been generally acceptable in the high-temperature regime, but significant deviations from theoretical values occur at low temperatures.<sup>5–7</sup> Approaches to address these discrepancies have been numerous,<sup>8–10</sup> but the most common have been based on the assumption that appreciable structural distortions in the complex occur at low temperature. Consequently, the availability of asymmetric  $\text{Cr}^{\text{III}}_3\text{O}$  complexes would be important in addressing this problem. Reports of unsymmetric members of this class of compounds are rare, limited to a few reports prior to 1930 in which the complexes are characterized essentially by only

elemental analysis<sup>11–13</sup> and one recent report in which the complex was more thoroughly but not structurally characterized.<sup>14</sup>

As part of a program to synthesize new  $\text{Cr}^{\text{III}}$  carboxylate complexes as models of the Cr-containing protein, low-molecular-weight chromium-binding substance,<sup>15,16</sup> procedures for the synthesis of unsymmetric  $\text{Cr}^{\text{III}}_3\text{O}$  complexes have been developed. Herein are reported the syntheses of  $\text{Cr}_3\text{O}(\text{O}_2\text{CPh})_6(\text{8-hqn})_3$  (1) and its acetate and 5-chloro-8-hydroxyquinoline (5-Cl-hqn) analogues and selected spectroscopic and magnetic properties of these species.

## Experimental Section

**Syntheses.** All manipulations were performed under aerobic conditions, and all chemicals were used as received. Elemental analyses were performed by Galbraith Laboratories, Knoxville, TN.  $[\text{Cr}_3\text{O}(\text{O}_2\text{CPh})_6(\text{H}_2\text{O})_3]\text{NO}_3 \cdot \text{H}_2\text{O}$ ,<sup>14</sup>  $[\text{Cr}_3\text{O}(\text{OAc})_6(\text{H}_2\text{O})_3]\text{Cl}$ ,<sup>17</sup> and 8-hqn-5,7- $d_2$ <sup>18</sup> were prepared as described in the literature or were available from previous work.

**$\text{Cr}_3\text{O}(\text{O}_2\text{CPh})_4(\text{8-hqn})_3 \cdot 1.25\text{CH}_2\text{Cl}_2$ .** A solution of 1.05 g (1.02 mmol)  $[\text{Cr}_3\text{O}(\text{O}_2\text{CPh})_6(\text{H}_2\text{O})_3]\text{NO}_3 \cdot \text{H}_2\text{O}$ , 0.44 g (3.0 mmol) of 8-hydroxyquinoline (8-hqnH), and 0.30 g (3.0 mmol) of  $\text{NET}_3$  in 45 mL of MeCN was heated to reflux for 2 1/2 h. After the mixture was allowed to cool, an olive-green solid was separated from a yellow-green solution by filtration. The solid was dissolved in  $\text{CH}_2\text{Cl}_2$ , and the resulting solution was layered with hexanes. After several days, dark crystals of 1·1.25 $\text{CH}_2\text{Cl}_2$  were collected by filtration in ca. 20% yield (based on Cr). Anal. Calcd (found) for  $\text{C}_{56.25}\text{H}_{40.5}\text{N}_3\text{O}_{12}\text{Cl}_{2.5}\text{Cr}_3$ : C, 56.53 (56.81); H, 3.42 (3.31); N, 3.52 (3.13); Cr, 13.05 (13.02). Selected IR data: 1625 (vs), 1580 (vs), 1570 (vs), 1515 (vs), 1335 (s), 1295 (m), 1280 (m), 1235 (w), 1185 (m), 1120 (s), 1075 (w), 1030 (m), 825 (m), 805 (m), 785 (m), 750 (m), 720 (vs), 680 (s), 645 (m), 635 (m), 570 (m), 535  $\text{cm}^{-1}$  (s). UV/vis (DMSO): 368 nm ( $\epsilon = 2.57 \times 10^3$ ), 598

<sup>®</sup> Abstract published in *Advance ACS Abstracts*, June 15, 1995.

- (1) University of Alabama.
- (2) University of New Orleans.
- (3) University of Virginia.
- (4) Cannon, R. D.; White, R. P. *Prog. Inorg. Chem.* **1988**, *36*, 195.
- (5) Schriempf, J. T.; Friedberg, S. A. *J. Chem. Phys.* **1964**, *40*, 296.
- (6) Earnshaw, A.; Figgis, B. N.; Lewis, J. *J. Chem. Soc. A* **1966**, 1656.
- (7) Zelentsov, V. V.; Zhemchuzhnikova, T. A.; Rakitin, Y. V.; Yablokov, Y. V.; Yablokov, K. M. *Koord. Khim.* **1975**, *1*, 194.
- (8) Tsukerblat, B. S.; Belinskii, M. I.; Kuyavskaya, B. Y. *Inorg. Chem.* **1983**, *22*, 995.
- (9) Jones, D. H.; Sams, J. R.; Thompson, R. C. *J. Chem. Phys.* **1984**, *81*, 440.
- (10) Wucher, J.; Wasscher, J. D. *Physica* **1954**, *20*, 721.
- (11) Weinland, R.; Lindner, J. Z. *Anorg. Allg. Chem.* **1930**, *190*, 285.
- (12) Weinland, R. F.; Hachenburg, H. Z. *Anorg. Allg. Chem.* **1923**, *126*, 285.
- (13) Werner, A. *Ber. Dtsch. Chem. Ges.* **1908**, *41*, 3447.
- (14) Harton, A.; Nagi, M. K.; Glass, M. M.; Junk, P. C.; Atwood, J. L.; Vincent, J. B. *Inorg. Chim. Acta* **1994**, *217*, 171.

- (15) Yamamoto, A.; Wada, O.; Ono, T. *Eur. J. Biochem.* **1987**, *165*, 627.
- (16) Vincent, J. B. In *Encyclopedia of Inorganic Chemistry*; King, R. B., Ed.; John Wiley & Sons: Chichester, U.K., 1994; pp 661–665.
- (17) Johnson, M. K.; Powell, D. B.; Cannon, R. D. *Spectrochim. Acta* **1981**, *37A*, 995.
- (18) Addy, P.; Evans, D. F.; deSouza, Q. *Polyhedron* **1987**, *6*, 1987.

**Table 1.** Crystallographic Data for Complex **1**·1.25CH<sub>2</sub>Cl<sub>2</sub><sup>a</sup>

chem formula Cr <sub>3</sub> Cl <sub>2</sub> O <sub>12</sub> N <sub>3</sub> C <sub>56</sub> H <sub>40</sub> <sup>a</sup>	fw 1173.84 <sup>a</sup>
<i>a</i> = 11.901(2) Å	space group <i>P</i> $\bar{1}$ (No. 2)
<i>b</i> = 19.410(4) Å	<i>T</i> = -110 °C
<i>c</i> = 11.701(1) Å	$\lambda$ = 0.710 69 Å
$\alpha$ = 96.58(1)°	$\rho_{\text{calcd}}$ = 1.492 g cm <sup>-3</sup>
$\beta$ = 95.66(1)°	$\mu$ = 7.64 cm <sup>-1</sup>
$\gamma$ = 101.21(1)°	<i>R</i> = 0.057 <sup>b</sup>
<i>V</i> = 2614(1) Å <sup>3</sup>	<i>R</i> <sub>w</sub> = 0.069 <sup>c</sup>
<i>Z</i> = 2	

<sup>a</sup> Assuming one molecule of solvate. <sup>b</sup>  $R = \sum(|F_o| - |F_c|) / \sum|F_o|$ .  
<sup>c</sup>  $R_w = (\sum w(|F_o| - |F_c|)^2 / \sum w|F_o|^2)^{1/2}$ .

(70.9). The O<sub>2</sub>CC<sub>6</sub>D<sub>5</sub> analogue was prepared from [Cr<sub>3</sub>O(O<sub>2</sub>CC<sub>6</sub>D<sub>5</sub>)<sub>6</sub>(H<sub>2</sub>O)<sub>3</sub>]NO<sub>3</sub>·H<sub>2</sub>O using an identical procedure. Selected IR data: 1615 (s), 1590 (s), 1530 (m), 1515 (s), 1330 (m), 1275 (m), 1235 (w), 1190 (w), 1115 (m), 1040 (w), 845 (m), 825 (m), 805 (m), 785 (m), 750 (m), 735 (m), 720 (m), 660 (m), 645 (m), 630 (m), 570 (w), 550 (m), 530 (m), 520 cm<sup>-1</sup> (m).

**Cr<sub>3</sub>O(O<sub>2</sub>CPh)<sub>4</sub>(5-Cl-8-hqn)<sub>3</sub>(2)·1.5C<sub>6</sub>H<sub>14</sub>.** This material was synthesized similarly to **1** but replacing the 8-hqnH with 5-Cl-8-hqnH (0.54 g, 3.0 mmol). The yield was similar to that of **1**. Anal. Calcd (found) for C<sub>66</sub>H<sub>52</sub>N<sub>3</sub>O<sub>12</sub>Cl<sub>3</sub>Cr<sub>3</sub>: C, 58.17 (57.89); H, 4.27 (3.58); N, 3.18 (3.17); Cr, 11.8 (11.32). Selected IR data: 1615 (s), 1570 (s), 1515 (s), 1335 (m), 1105 (m), 845 (m), 800 (m), 775 (m), 735 (m), 690 (m), 650 cm<sup>-1</sup> (m). UV/vis (DMSO): 368 nm ( $\epsilon = 2.91 \times 10^3$ ), 598 (75.7).

**Cr<sub>3</sub>O(OAc)<sub>4</sub>(8-hqn)<sub>3</sub>(3)<sup>2/3</sup>CH<sub>2</sub>Cl<sub>2</sub>.** A solution of 2.00 g (3.25 mmol) of [Cr<sub>3</sub>O(OAc)<sub>6</sub>(H<sub>2</sub>O)<sub>3</sub>]Cl and 0.71 g (4.87 mmol) of 8-hqnH in 45 mL of MeCN was heated to reflux for 1 1/2 h. After the mixture was allowed to cool, a deep green solid was isolated by filtration. The solid was recrystallized from a CH<sub>2</sub>Cl<sub>2</sub> solution layered with hexanes to give **3**<sup>2/3</sup>CH<sub>2</sub>Cl<sub>2</sub> in ca. 15% yield (based on Cr). Anal. Calcd (found) for Cr<sub>3</sub>N<sub>3</sub>C<sub>35.67</sub>H<sub>31.33</sub>O<sub>12</sub>Cl<sub>1.33</sub>Cr<sub>3</sub>: C, 47.75 (47.76); H, 3.52 (3.63); N, 4.68 (4.94); Cr, 17.39 (17.46). Selected IR data: 1610 (vs), 1580 (vs), 1325 (m), 1280 (m), 1235 (w), 1180 (w), 1110 (m), 1030 (w), 820 (m), 805 (m), 785 (m), 750 (s), 740 (s), 720 (s), 670 (m), 650 (m), 630 (m), 560 (m), 530 (s), 435 cm<sup>-1</sup> (w). UV/vis (DMSO): 432 nm ( $\epsilon = 2.87 \times 10^3$ ), 532 (846), 598 (760). The O<sub>2</sub>CCD<sub>3</sub> analogue was prepared from [Cr<sub>3</sub>O(O<sub>2</sub>CCD<sub>3</sub>)<sub>6</sub>(H<sub>2</sub>O)<sub>3</sub>]Cl using an identical procedure. Selected IR data: 1600 (vs), 1560 (s), 1510 (s), 1330 (m), 1290 (w), 1235 (w), 1180 (w), 1155 (w), 1120 (m), 1035 (w), 930 (m), 850 (m), 825 (m), 805 (m), 785 (m), 750 (s), 730 (s), 695 (m), 645 (s), 630 (sh), 610 (m), 530 (m), 430 cm<sup>-1</sup> (w).

**Physical Measurements.** Infrared spectra (Nujol mull) were recorded on a Perkin-Elmer 283 B spectrophotometer. <sup>1</sup>H and <sup>2</sup>H NMR spectra were obtained using a Bruker AM-360 and a Bruker AM-500 spectrometer, respectively, at ca. 23 °C. Chemical shifts are reported on the  $\delta$  scale (shifts downfield are positive) using the solvent protio or deuterio impurity signal(s) as a reference. A Hewlett-Packard 8451A spectrophotometer was used to record ultraviolet/visible spectra. Electron impact mass spectra were obtained using a VG Autospec high-resolution mass spectrometer. EPR spectra were recorded on a Varian E-12 spectrophotometer equipped with an Oxford ESR 900 cryostat.

Magnetic susceptibility data were recorded with an SHE Corp. VTS superconducting SQUID susceptometer. The sample bucket was fabricated from an Al-Si alloy obtained from the SHE Corp. The magnetic susceptibility of the sample bucket was measured independently over the temperature region 8–300 K, and the magnetic data for all samples were then corrected for the bucket contribution. Magnetic data were recorded on polycrystalline samples weighing 100 mg or so. The samples were measured at 2.5 kOe. Measurement and calibration procedures are reported elsewhere.<sup>19</sup> The magnetic susceptibility data corrected for diamagnetism by using Pascal's constants are calculated as trimer susceptibility (i.e., three Cr<sup>III</sup> ions per molecule) as a function of temperature. The diamagnetic corrections for **1**, Cr<sub>3</sub>O(O<sub>2</sub>CPh)<sub>4</sub>(8-hqn)<sub>3</sub>·1.25CH<sub>2</sub>Cl<sub>2</sub>, and **3**, Cr<sub>3</sub>O(OAc)<sub>4</sub>(8-hqn)<sub>3</sub><sup>2/3</sup>CH<sub>2</sub>Cl<sub>2</sub> are 0.000 54 and 0.000 37 emu/mol, respectively.

**X-ray Crystallography and Structure Solution.** All X-ray measurements were carried out on a Rigaku AFC6S diffractometer at -110 °C using MoK $\alpha$  radiation ( $\lambda = 0.710 69$  Å). A summary of the

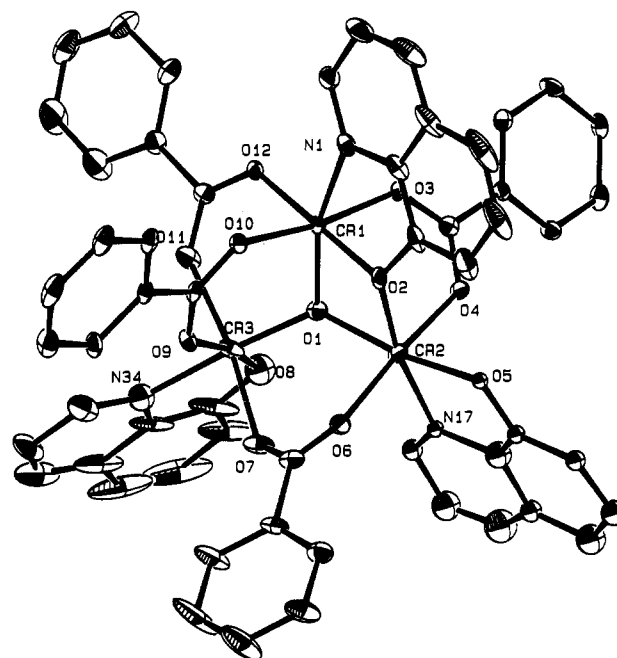


**Figure 1.** Structure of complex **1** showing the atom-labeling scheme. Carbon atoms are labeled consecutively from N and O atoms. H atoms have been omitted for clarity.

experimental and structure solution procedure is given in Table 1. Lattice parameters were determined by the least-squares refinement of 25 high-angle reflections. Intensities of three standard reflections measured every 100 reflections showed no significant changes. An empirical absorption correction was applied by using  $\psi$  scans of several reflections with the  $\chi$  angle close to 90°. The transmission factors were in the range 0.81–1.00. All calculations pertinent to the structure solution and refinement were performed on a VAXstation 3520 computer using the TEXSAN 5.0 software.<sup>20</sup> The structure was solved by direct methods (SIR88).<sup>21</sup> Full-matrix least-squares refinement with anisotropic thermal displacement parameters for all non-hydrogen atoms but those belonging to one of the 8-hydroxyquinoline ligands yielded the final *R* of 0.057 (*R*<sub>w</sub> = 0.069).

Some of the ligands and especially those coordinated to the Cr(2) and Cr(3) atoms showed somewhat higher than usual thermal parameters, indicating possible disorder. The disorder was successfully resolved for the 8-hydroxyquinoline ligand O(5), N(17) which were found in two slightly different orientations with occupancy factors of 0.5. The atoms belonging to the ligand were refined with isotropic thermal displacement parameters.

The final difference map showed a peak of the height 1.41 e/A<sup>3</sup> in the vicinity of the disordered 8-hydroxyquinoline moiety. The final atomic coordinates are presented in Table 2.

**Synthesis.** In an effort to synthesize multinuclear chromium assemblies, this laboratory has been examining the reaction of trinuclear oxo-centered complexes of the general form [Cr<sup>III</sup><sub>3</sub>(O<sub>2</sub>CR)<sub>6</sub>(L)<sub>3</sub>]<sup>+</sup>X<sup>-</sup> (where L is a monodentate ligand) in organic solvents.<sup>22,23</sup> Previously, this procedure using 2,2'-bipyridine,<sup>22</sup> 1,10-phenanthroline,<sup>22</sup> and picolinate<sup>23</sup> (and their derivatives) has resulted in the formation of tetranuclear assemblies. The terminal monodentate ligands of the starting trinuclear materials are somewhat labile;<sup>14</sup> thus, the reactions probably proceed via substitution of the terminal monodentate ligand (L) with one of the metal-binding moieties of the bidentate ligands.

(20) TEXSAN: Single Crystal Structure Analysis Software, Version 5.0; Molecular Structure Corp.: The Woodlands, TX 77381, 1989.

(21) SIR88: Burla, M. C.; Camalli, M.; Cascarano, G.; Giacovazzo, C.; Polidori, G.; Spagna, R.; Viterbo, D. *J. Appl. Crystallogr.* **1989**, *22*, 389.

(22) Ellis, T.; Glass, M.; Harton, A.; Folting, K.; Huffman, J.; Vincent, J. B. *Inorg. Chem.* **1994**, *33*, 5522. Bino, A.; Chayat, R.; Pedersen, E.; Schneider, A. *Inorg. Chem.* **1991**, *30*, 856.

(23) Donald, S.; Terrell, K.; Vincent, J. B.; Robinson, K. D. *Polyhedron* **1995**, *14*, 971.

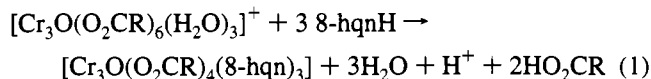
**Table 2.** Selected Fractional Coordinates and Isotropic Parameters for Complex **1**·1.25CH<sub>2</sub>Cl<sub>2</sub>

atom	x	y	z	B(eq), <sup>a</sup> Å <sup>2</sup>	atom	x	y	z	B(eq), <sup>a</sup> Å <sup>2</sup>
Cr(1)	0.25545(8)	0.25300(5)	0.45941(8)	1.42(4)	C(20)	0.4156(8)	0.4225(5)	1.0513(8)	5.5(2)
Cr(2)	0.2465(1)	0.30235(5)	0.70203(9)	2.73(5)	C(20B)	0.526(2)	0.418(1)	1.044(2)	5.0(4)
Cr(3)	0.43290(8)	0.19231(6)	0.6290(1)	2.26(4)	C(21)	0.2272(7)	0.4508(5)	1.0963(7)	4.5(2)
Cl(1)	0.8367(2)	0.4485(2)	0.1925(3)	7.5(1)	C(21B)	0.350(2)	0.452(1)	1.116(2)	6.7(5)
Cl(2)	1.0535(2)	0.4990(2)	0.3448(3)	7.9(1)	C(22)	0.109(1)	0.4415(8)	1.051(1)	3.1(3)
O(1)	0.3462(3)	0.2619(2)	0.6043(3)	2.0(2)	C(23)	0.066(1)	0.4011(6)	0.943(1)	2.0(2)
O(2)	0.1349(4)	0.2640(2)	0.5591(3)	2.0(2)	C(23B)	0.161(1)	0.411(1)	0.988(1)	4.5(4)
O(3)	0.2970(3)	0.3565(2)	0.4569(3)	1.7(2)	C(24)	0.144(1)	0.3716(6)	0.880(1)	1.6(2)
O(4)	0.2867(4)	0.3942(2)	0.6441(3)	2.5(2)	C(25)	0.2388(7)	0.3792(4)	0.9146(6)	3.5(2)
O(5)	0.1062(7)	0.3346(4)	0.7707(7)	1.3(1)	C(25B)	0.333(1)	0.3809(7)	0.929(1)	2.5(3)
O(5B)	0.1627(8)	0.3432(5)	0.8062(8)	2.1(2)	C(26)	0.301(1)	0.4202(7)	1.029(1)	2.4(2)
O(6)	0.2124(4)	0.2149(2)	0.7755(4)	2.6(2)	C(27)	0.2838(6)	0.1801(3)	0.8134(5)	2.4(3)
O(7)	0.3843(4)	0.1824(2)	0.7860(4)	2.8(2)	C(28)	0.2438(6)	0.1336(3)	0.9013(5)	2.6(3)
O(8)	0.5707(5)	0.2627(3)	0.6952(5)	4.8(1)	C(29)	0.1483(6)	0.1428(4)	0.9549(6)	2.9(3)
O(9)	0.3068(3)	0.1087(2)	0.5733(4)	2.0(2)	C(30)	0.1070(7)	0.0975(5)	1.0312(7)	4.2(3)
O(10)	0.2002(3)	0.1486(2)	0.4368(3)	1.7(2)	C(31)	0.1584(9)	0.0432(6)	1.053(1)	7.5(6)
O(11)	0.4821(4)	0.1862(2)	0.4697(4)	2.9(2)	C(32)	0.254(1)	0.0335(7)	0.999(1)	9.3(7)
O(12)	0.3730(3)	0.2398(2)	0.3558(3)	1.8(2)	C(33)	0.2994(7)	0.0795(5)	0.9234(7)	4.9(4)
N(1)	0.1227(4)	0.2580(3)	0.3322(4)	2.0(2)	C(35)	0.5220(7)	0.0546(5)	0.6502(7)	4.8(4)
N(17)	0.328(1)	0.3499(5)	0.8515(9)	1.4(2)	C(36)	0.605(1)	0.0161(6)	0.692(1)	7.0(6)
N(17B)	0.388(1)	0.3459(6)	0.846(1)	2.0(2)	C(37)	0.705(1)	0.052(1)	0.752(1)	9.8(9)
N(34)	0.5412(5)	0.1238(4)	0.6686(5)	3.6(1)	C(38)	0.832(1)	0.176(1)	0.836(1)	12(1)
C(2)	0.1225(6)	0.2561(4)	0.2182(6)	2.7(3)	C(39)	0.844(1)	0.242(1)	0.845(2)	12(1)
C(3)	0.0263(7)	0.2677(4)	0.1480(6)	3.8(3)	C(40)	0.7591(7)	0.2771(7)	0.7984(7)	7.7(5)
C(4)	-0.0670(7)	0.2822(5)	0.1970(8)	4.5(4)	C(41)	0.6584(6)	0.2348(6)	0.7395(7)	5.6(4)
C(5)	-0.1585(7)	0.3040(5)	0.379(1)	6.2(5)	C(42)	0.6427(7)	0.1615(6)	0.7295(7)	5.1(4)
C(6)	-0.1490(8)	0.3074(5)	0.495(1)	6.3(5)	C(43)	0.7279(9)	0.125(1)	0.7737(8)	7.4(6)
C(7)	-0.0510(7)	0.2969(4)	0.5608(7)	4.1(3)	C(44)	0.2260(5)	0.1001(3)	0.4910(5)	1.6(2)
C(8)	0.0382(6)	0.2802(3)	0.5056(6)	2.6(3)	C(45)	0.1564(5)	0.0267(3)	0.4549(5)	1.9(2)
C(9)	0.0307(5)	0.2748(3)	0.3832(6)	2.6(3)	C(46)	0.1840(6)	-0.0297(3)	0.5111(6)	2.5(3)
C(10)	-0.0679(6)	0.2861(4)	0.3160(8)	4.0(3)	C(47)	0.1203(7)	-0.0980(4)	0.4737(7)	3.5(3)
C(11)	0.3069(5)	0.4048(3)	0.5416(5)	1.9(2)	C(48)	0.0304(7)	-0.1103(4)	0.3834(7)	3.7(3)
C(12)	0.3439(5)	0.4796(3)	0.5219(5)	1.6(2)	C(49)	0.0025(6)	-0.0549(4)	0.3303(6)	3.0(3)
C(13)	0.3418(6)	0.4966(3)	0.4112(5)	2.6(3)	C(50)	0.0665(5)	0.0140(3)	0.3654(6)	2.2(2)
C(14)	0.3777(6)	0.5667(3)	0.3919(6)	2.7(3)	C(51)	0.4535(5)	0.2080(3)	0.3750(5)	2.1(2)
C(15)	0.4147(5)	0.6188(3)	0.4839(6)	2.1(2)	C(52)	0.5219(6)	0.1929(4)	0.2774(6)	2.6(3)
C(16)	0.4157(6)	0.6020(3)	0.5960(6)	2.5(3)	C(53)	0.6107(7)	0.1564(5)	0.2912(8)	5.4(4)
C(17)	0.3798(5)	0.5331(3)	0.6149(5)	2.0(2)	C(54)	0.6709(8)	0.1422(6)	0.201(1)	6.5(5)
C(18)	0.441(1)	0.3579(7)	0.887(1)	2.1(3)	C(55)	0.6459(7)	0.1642(5)	0.0960(8)	4.8(4)
C(18B)	0.499(1)	0.3465(7)	0.856(1)	1.9(2)	C(56)	0.5586(7)	0.2001(5)	0.0812(6)	4.3(3)
C(19)	0.489(2)	0.395(1)	0.999(2)	4.3(4)	C(57)	0.4951(6)	0.2151(4)	0.1713(6)	3.2(3)
C(19B)	0.573(1)	0.3825(8)	0.962(1)	3.2(3)	C(58)	0.9058(8)	0.5027(5)	0.323(1)	7.1(5)

<sup>a</sup> The equivalent isotropic temperature factor is defined as  $8\pi^2/3 \sum_{i=1}^3 \sum_{j=1}^3 U_{ij} a_i^* a_j^* \bar{a}_i \bar{a}_j$ .

Accommodation of the second metal-binding moiety then probably initiates reorganization or the assembly. However, the use of the bidentate ligand 8-hydroxyquinoline (8-hqnH) leads to different results.

Treatment of green solutions or slurries of the starting trinuclear species in MeCN with 8-hqnH or [NEt<sub>3</sub>H][8-hqn] followed by heating to reflux results in a color change to yellow-green, indicative of the formation of the unsymmetric trinuclear species, and in formation of a green solid. The procedure is summarized in eq 1. The balanced



equation suggests that the reaction involves simple displacement of H<sub>2</sub>O and a portion of the bridging carboxylates with replacement by 8-hqn; the parent Cr<sub>3</sub>O core appears to be maintained.

For complex **3**, the acetate derivative, use of the small 8-hqnH:Cr<sub>3</sub>O ratio is necessary to minimize formation of the tris chelate complex Cr(8-hqn)<sub>3</sub>.

### Description of Structure

The structure of complex **1** is shown in Figure 1. Selected atomic coordinates and interatomic distances and angles are listed in Tables 2 and 3, respectively. The complex crystallizes in the triclinic space group *P*1̄, with the molecule possessing no imposed symmetry elements.

The core of the complex consists of a scalene triangle of chromic centers with a central μ<sub>3</sub>-oxide. The unsymmetric nature of the core is emphasized by the chromium--chromium separations (2.909(1), 3.235(1), and 3.466(2) Å) and the chromium--oxo--chromium angles (94.4(2), 118.1(2), and 130.2(2)°). This is in stark contrast to the [Cr<sub>3</sub>O]<sup>7+</sup> cores of "basic carboxylate" type trinuclear chromic species, as shown by the metric parameters of the only structurally-characterized member of this class with benzoate ligands in Table 4.<sup>14</sup> This latter complex possesses a C<sub>3</sub> axis perpendicular to the Cr<sub>3</sub>O plane, imposing D<sub>3h</sub> symmetry onto the core. The different chromium--chromium separations are manifested by the types of ligands bridging the sets of chromic ions. The shortest distance (2.909(1) Å) is spanned by a bridging benzoate ligand and a bridging phenoxide-like oxygen from an 8-hqn ligand. The intermediate distance (3.235(1) Å) is spanned by two bridging benzoate ligands; this distance is very similar to that of the symmetric benzoate complex (3.263(9) Å),<sup>14</sup> where each pair of chromium centers is bridged by two benzoate ligands. A single benzoate bridges across the long chromium--chromium separation (3.466(2) Å).

The remaining coordination sites are filled by two chelating 8-hqn ligands and by the nitrogen of the η<sup>2</sup>-μ<sub>2</sub>-8-hqn ligand (which also provides the bridging phenoxide group).

**Table 3.** Selected Interatomic Distances (Å) and Angles (deg) for Complex 1·1.25CH<sub>2</sub>Cl<sub>2</sub>

a. Distances			
Cr(1)–O(1)	1.890(4)	Cr(3)–O(1)	1.882(4)
Cr(1)–O(2)	1.963(4)	Cr(3)–O(7)	1.998(4)
Cr(1)–O(3)	1.978(4)	Cr(3)–O(8)	1.947(6)
Cr(1)–O(10)	1.983(4)	Cr(3)–O(9)	1.982(4)
Cr(1)–O(12)	1.973(4)	Cr(3)–O(11)	2.006(5)
Cr(1)–N(1)	2.085(5)	Cr(3)–N(34)	2.081(6)
Cr(2)–O(1)	1.939(4)		
Cr(2)–O(2)	2.002(4)	Cr(1)–Cr(2)	2.909(1)
Cr(2)–O(4)	1.969(4)	Cr(1)–Cr(3)	3.235(1)
Cr(2)–O(5)	2.093(8)	Cr(2)–Cr(3)	3.466(2)
Cr(2)–O(5B)	1.854(9)		
Cr(2)–O(6)	1.980(4)		
Cr(2)–N(17)	1.95(1)		
Cr(2)–N(17B)	2.23(1)		
O(12)–C(51)	1.253(7)	O(9)–C(44)	1.263(7)
O(11)–C(51)	1.270(7)	O(10)–C(44)	1.262(7)
O(6)–C(27)	1.262(8)	O(3)–C(11)	1.263(7)
O(7)–C(27)	1.263(8)	O(4)–C(11)	1.277(7)
b. Angles			
O(1)–Cr(1)–O(2)	82.0(2)	O(2)–Cr(2)–N(17)	167.5(4)
O(1)–Cr(1)–O(3)	91.2(2)	O(2)–Cr(2)–N(17B)	172.7(3)
O(1)–Cr(1)–O(10)	98.0(2)	O(4)–Cr(2)–O(5)	89.6(2)
O(1)–Cr(1)–O(12)	99.4(2)	O(4)–Cr(2)–O(5B)	88.9(3)
O(1)–Cr(1)–N(1)	162.0(2)	O(4)–Cr(2)–O(6)	174.4(2)
O(2)–Cr(1)–O(3)	91.5(2)	O(4)–Cr(2)–N(17)	87.0(3)
O(2)–Cr(1)–O(10)	90.3(2)	O(4)–Cr(2)–N(17B)	86.6(3)
O(2)–Cr(1)–O(12)	178.2(2)	O(5)–Cr(2)–O(5B)	20.3(3)
O(2)–Cr(1)–N(1)	81.0(2)	O(5)–Cr(2)–O(6)	89.0(2)
O(3)–Cr(1)–O(10)	170.8(2)	O(5)–Cr(2)–N(17)	82.5(4)
O(3)–Cr(1)–O(12)	89.5(2)	O(5)–Cr(2)–N(17B)	101.4(4)
O(3)–Cr(1)–N(1)	83.4(2)	O(5B)–Cr(2)–O(6)	87.9(3)
O(10)–Cr(1)–O(12)	88.5(2)	O(5B)–Cr(2)–N(17)	62.2(4)
O(10)–Cr(1)–N(1)	88.0(2)	O(5B)–Cr(2)–N(17B)	81.1(4)
O(12)–Cr(1)–N(1)	97.7(2)	O(6)–Cr(2)–N(17)	87.5(3)
O(1)–Cr(2)–O(2)	79.8(2)	O(6)–Cr(2)–N(17B)	88.4(3)
O(1)–Cr(2)–O(4)	91.3(2)	O(1)–Cr(3)–O(7)	93.1(2)
O(1)–Cr(2)–O(5)	165.0(3)	O(1)–Cr(3)–O(8)	92.8(2)
O(1)–Cr(2)–O(5B)	174.7(3)	O(1)–Cr(3)–O(9)	96.9(2)
O(1)–Cr(2)–O(6)	91.4(2)	O(1)–Cr(3)–O(11)	94.4(2)
O(1)–Cr(2)–N(17)	112.5(4)	O(1)–Cr(3)–N(34)	173.8(2)
O(1)–Cr(2)–N(17B)	93.6(3)	O(7)–Cr(3)–O(8)	91.5(2)
O(2)–Cr(2)–O(4)	90.4(2)	O(7)–Cr(3)–O(9)	85.6(2)
O(2)–Cr(2)–O(5)	85.3(3)	O(7)–Cr(3)–O(11)	171.1(2)
O(2)–Cr(2)–O(5B)	105.5(3)	O(7)–Cr(3)–N(34)	85.2(2)
O(2)–Cr(2)–O(6)	94.9(2)	O(8)–Cr(3)–O(9)	170.0(2)
Cr(1)–O(1)–Cr(2)	98.9(2)	O(8)–Cr(3)–O(11)	93.0(2)
Cr(1)–O(1)–Cr(3)	118.1(2)	O(8)–Cr(3)–N(34)	81.3(2)
Cr(2)–O(1)–Cr(3)	130.2(2)	O(9)–Cr(3)–O(11)	88.8(2)
Cr(1)–O(2)–Cr(2)	94.4(2)	O(9)–Cr(3)–N(34)	88.9(2)
		O(11)–Cr(3)–N(34)	87.8(2)
Cr(1)–O(3)–C(11)	127.0(4)	Cr(2)–O(4)–C(11)	127.3(4)
Cr(2)–O(6)–C(27)	127.1(4)	Cr(3)–O(9)–C(44)	129.5(4)
Cr(3)–O(7)–C(27)	126.2(4)	Cr(3)–O(11)–C(51)	136.2(4)
Cr(1)–O(10)–C(44)	132.9(4)	Cr(1)–O(12)–C(51)	125.8(4)
O(3)–C(11)–O(4)	124.8(6)	O(6)–C(27)–O(7)	126.2(6)
O(9)–C(44)–O(10)	125.2(5)	O(11)–C(51)–O(12)	125.9(6)

### Magnetic Susceptibility Studies

The magnetic susceptibility data for the two complexes are shown in Figures 2 and 3 as the effective magnetic moment ( $\mu_{\text{eff}}$ ) plotted as a function of temperature and in the supporting information as inverse magnetic susceptibility plotted as a function of temperature.

The general feature of the magnetic data for both complexes is approximate for a trimer with antiferromagnetic exchange within the chromium(III) trimeric unit. Thus the temperature dependence of the reciprocal susceptibility follows the Curie–Weiss law at high temperatures ( $T > 100$  K), exhibits non-Curie–Weiss behavior at intermediate temperatures ( $15 \text{ K} < T < 100$  K), and again exhibits Curie–Weiss behavior at the lowest temperatures ( $T < 15$  K), but with a reduced effective

**Table 4.** Comparison of Selected Structural Parameters for Symmetric and Unsymmetric [Cr<sub>3</sub>O]<sup>7+</sup> Complexes

parameter	1	[Cr <sub>3</sub> O(O <sub>2</sub> CPh) <sub>6</sub> (py) <sub>3</sub> ] <sup>+</sup>
Cr–Cr, Å	2.909(1)	3.263(8)
	3.235(1)	
	3.466(2)	
Cr–O <sup>2-</sup> , Å	1.890(4)	1.883(4)
	1.939(4)	
	1.882(4)	
Cr–O <sub>2</sub> Cr, Å	1.969(4)	1.96(2)
	–2.006(5)	2.00(1)
Cr–N, Å	2.085(5)	2.245(2)
	1.95(1), 2.23(1)	
	2.081(6)	
Cr–O <sup>2-</sup> –Cr, deg	98.9(2)	120.0 <sup>a</sup>
	118.1(2)	
	130.2(2)	
ref	this work	14

<sup>a</sup> Symmetry imposed.

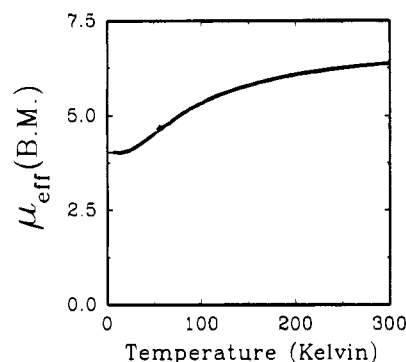


**Figure 2.** Effective magnetic moment ( $\mu_{\text{eff}} = (8\chi T)^{1/2}$ ) plotted as a function of temperature for 1·1.25CH<sub>2</sub>Cl<sub>2</sub>. The smooth curve drawn through the points is the least-squares fit of the data using eq 4 as described in the text.

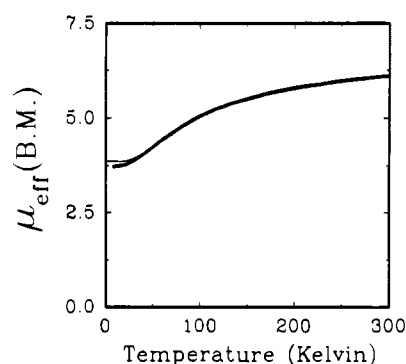


**Figure 3.** Effective magnetic moment ( $\mu_{\text{eff}} = (8\chi T)^{1/2}$ ) plotted as a function of temperature for 3·2/3CH<sub>2</sub>Cl<sub>2</sub>. The smooth curve drawn through the points is the least-squares fit of the data using eq 4 as described in the text.

spin value. The magnetic susceptibility data in the high- and low-temperature limits was fit with the Curie–Weiss expression

$$\chi = \frac{C}{T - \Theta} = \frac{Ng^2\mu_B^2 S(S+1)}{3k(T - \Theta)} \quad (2)$$

where  $S = 3/2$  for chromium(III) and all of the other parameters have their usual meaning. The least-squares-fitted parameters are listed in Table 5. The high-temperature Curie constant and  $g$  values are averages for the three chromium(III) ions of the trimeric unit, while the low-temperature values are for the trimer as a whole. The magnitude of the Curie constant determined for the low-temperature analyses requires a single spin  $S = 3/2$  ground state for the entire trimer.

**Table 5.** Magnetic Parameters for  $1 \cdot 1.25\text{CH}_2\text{Cl}_2$  and  $3 \cdot 2/3\text{CH}_2\text{Cl}_2$ 

Curie-Weiss Parameters				
compound	temp region, K	$K$	emu $\Theta$ , K/mol	$C$
1, $\text{Cr}_3\text{O}(\text{O}_2\text{CPh})_4(8\text{-hq})_3 \cdot 1.25\text{CH}_2\text{Cl}_2$	75–300	–81	6.46	2.14
	8–15	–0.1	2.04	2.09
3, $\text{Cr}_3\text{O}(\text{OAc})_4(8\text{-hq})_3 \cdot 0.66\text{CH}_2\text{Cl}_2$	75–300	–88	6.02	2.07
	8–15	–0.2	1.77	1.95

Trimer Parameters				
compound	temp region, K	$J/k$ , K	$g$	
1, $\text{Cr}_3\text{O}(\text{O}_2\text{CPh})_4(8\text{-hq})_3 \cdot 1.25\text{CH}_2\text{Cl}_2$	8–300	–4.6	2.08	
3, $\text{Cr}_3\text{O}(\text{OAc})_4(8\text{-hq})_3 \cdot 0.66\text{CH}_2\text{Cl}_2$	8–300	–5.1	2.01	

From the Curie-Weiss relationship with  $S = 3/2$  for each of the three  $\text{Cr}^{\text{III}}$  ions, an average of the three  $g$  values of 2.14 was obtained for  $1 \cdot 1.25\text{CH}_2\text{Cl}_2$ . At 300 K, the magnetic moment for **1** is  $6.36 \mu_{\text{B}}$  per trimer or  $3.67 \mu_{\text{B}}$  per chromium(III) ion, which is only slightly less than the value 3.87 observed for  $\text{Cr}^{\text{III}}$  systems without magnetic coupling. This indicates that the magnetic coupling in the complex is not strong enough to significantly depopulate the higher magnetic energy levels at room temperatures. The magnetic moments of both complexes decrease slowly as temperatures decrease down to 15 K. Below 15 K, the magnetic moment varies little with the temperature and is  $4.0 \mu_{\text{B}}$  per trimer (**1**), which is appropriate for a system with a spin  $3/2$  ground state. That is, the three spins  $S = 3/2$  of the chromium(III) ions have coupled together to yield a net spin angular momentum that can be represented as a single spin  $S = 3/2$  for the trimer molecule as a whole in the strong antiferromagnetic exchange interaction limit. At low temperatures ( $T < 15$  K), the temperature dependence of the reciprocal susceptibility becomes linear and the data extrapolate to a Weiss constant  $\Theta$  of  $-0.1$  K. The source of this Weiss constant is probably a zero-field splitting of the  $S = 3/2$  trimer ground state. The depopulation of high-spin paramagnetic states to low-spin paramagnetic states for a trimeric material is observed in some other trimer  $\text{Cr}(\text{III})$  systems, for example,  $\text{Cr}_3(\text{C}_{17}\text{H}_{12}\text{O}_3)_2(\text{H}_2\text{O})_3(\text{OH})_5^{24}$  and  $[(\text{C}_6\text{H}_5)_4\text{P}]_3[\text{Cr}_3\text{Se}_{24}]^{25}$ .

We have fit the magnetic data over the entire temperature range to a theoretical model using the trimeric spin Hamiltonian

$$\mathcal{H} = -2J[\mathbf{S}_1 \cdot \mathbf{S}_2 + \mathbf{S}_2 \cdot \mathbf{S}_3] - 2J'\mathbf{S}_1 \cdot \mathbf{S}_3 \quad (3)$$

A dissymmetric exchange field is required from the results of the Curie-Weiss analysis. If only one  $J$  value is used, as for a symmetric equilateral trimer, there is a ground state doublet. The Curie-Weiss analysis clearly shows a ground state quartet, which requires more than one  $J$  value. Using the spin product basis set of wave functions ( $\Psi = |m_{S1}, m_{S2}, m_{S3}\rangle$ ), a total of 64 wave functions are obtained. The action of the spin Hamiltonian (eq 3) on these wave functions yields 12 energy levels distributed with coupled spin quantum numbers as follows:  $S_T = 9/2$  (1),  $7/2$  (2),  $5/2$  (3),  $3/2$  (4),  $1/2$  (2), where the numbers in parentheses represent the numbers of the  $S_T$  states with the corresponding quantum number. The energy levels were determined by diagonalizing the  $\mathbf{H}_{ij}$  matrix ( $\mathbf{H}_{ij} = \langle \Psi_i | \mathcal{H} | \Psi_j \rangle$ ). The diagonalization was simplified by block-factoring the matrix into  $M_{ST}$  submatrices, where  $M_{ST} = m_{S1} + m_{S2} + m_{S3}$ . Since the spin Hamiltonian illustrated in eq 3 is isotropic, a modified form of the Van Vleck equation may be used which neglects

the higher order cross-diagonal terms. The magnetic susceptibilities of the trimer were calculated from the spin-coupled wave functions using the modified Van Vleck equation<sup>26</sup>

$$\chi = \frac{N}{H} \frac{\sum_{i=1,n} \frac{|\langle \Psi_i | \hat{\mu} | \Psi_i \rangle|^2}{kT} e^{-E_i/kT}}{\sum_{i=1,n} e^{-E_i/kT}} \quad (4)$$

where  $E_i$  is the energy of the states with wave function  $\Psi_i$  and  $\hat{\mu}$  is the moment operator ( $\hat{m} = g\mu_{\text{B}}\hat{S}_z$ ).

When  $J$  and  $J'$  were allowed to vary independently,  $J'$  tended toward a very small value that is necessary to give the proper distribution of energy levels (i.e., a ground state quartet). Therefore, fits were attempted with  $J'$  fixed at zero. These fits were as good as those that allowed  $J'$  to vary, and the values with  $J'$  set to zero are therefore reported since only one coupling parameter is used. The results of a least-squares fit of the magnetic data are illustrated in Figures 2 and 3 as plots of the effective magnetic moment ( $\mu_{\text{eff}} = (8\chi T)^{1/2}$ ) for the two complexes, respectively. The smooth curve drawn through the points represents the best fit of the trimer model using the fitted parameters listed in Table 5.

It is concluded that the pairs of chromium centers are antiferromagnetically coupled according to the symmetric isosceles trimer model with  $J'$  restricted to be zero and with both complexes exhibiting a ground state consistent with the coupled total spin of  $S = 3/2$  for the trimer as a whole. Other authors have often used a biquadratic term to analyze magnetically coupled chromium(III) systems.<sup>27</sup> This term was not needed for our analysis since we obtained acceptable fits with the unmodified spin Hamiltonian given in eq 4. Any improvement of the fit that would occur upon the addition of more terms to the spin Hamiltonian could be attributed to overparameterization.

The value determined for  $J'$  in both cases is slightly smaller than those determined for symmetric  $\text{Cr}_3\text{O}$  complexes, 6.5–11 K.<sup>4</sup> In these oxo-centered trinuclear complexes, it is very likely that the majority of this interaction is propagated by the oxide bridge, not the other bridging ligands; thus, the covalent framework of the unsymmetric complexes would suggest that all the chromic centers should be magnetically interacting. For coupled  $d^3$  centers, a Cr–O–Cr angle of  $180^\circ$  should maximize pathways for antiferromagnetic exchange while the number of ferromagnetic pathway increases as the angle approaches  $90^\circ$ .<sup>28</sup> Hence, this would suggest the weak magnetic coupling ( $J \sim 0$ ) might be that between Cr(1) and Cr(2) of complex **1** (Cr(1)–O(1)–Cr(2),  $98.9(2)^\circ$  vs  $118.1(2)^\circ$ , Cr(1)–O(1)–Cr(3), and  $130.2(2)^\circ$ , Cr(2)–O(1)–Cr(3)); yet, Cr(1) and Cr(2) are the only centers connected by two single-atom bridges, oxide O(1) and phenoxide O(2), which would be expected to increase magnetic interactions between these two chromic centers. Consequently, relating the magnetic properties of complexes **1** and **2** to their structure is difficult at present.

Interestingly, a similar situation has been observed in iron chemistry.  $[\text{Fe}_3(\mu_3\text{-O})(\text{TIEO})_2(\text{O}_2\text{CPh})_2\text{Cl}_3]$  (TIEO = 1,1,2-tris-(*N*-methylimidazol-2-yl)-1-hydroxyethane) contains a scalene triangle of iron atoms.<sup>29</sup> Variable magnetic susceptibility data

(26) van Vleck, J. H. *The Theory of Electric and Magnetic Susceptibilities*; Oxford University Press: London, 1932.

(27) Hodgson, D. J. In *Magneto-Structural Correlations in Exchange Coupled Systems*; Willer, R. D., Gatteschi, D., Khan, O., Eds.; Reidel: Dordrecht, Holland, 1983; p 497.

(28) Ginsberg, A. P. *Inorg. Chim. Acta Rev.* **1971**, 5, 45.

(24) Borer, L. L.; Horsma, R.; Rajan, O. A.; Sinn, E. *Inorg. Chem.* **1986**, 25, 3652.

(25) Zhang, J. H.; Flomer, W. A.; Kolis, J. W.; O'Connor, C. J. *Inorg. Chem.* **1990**, 29, 1108.

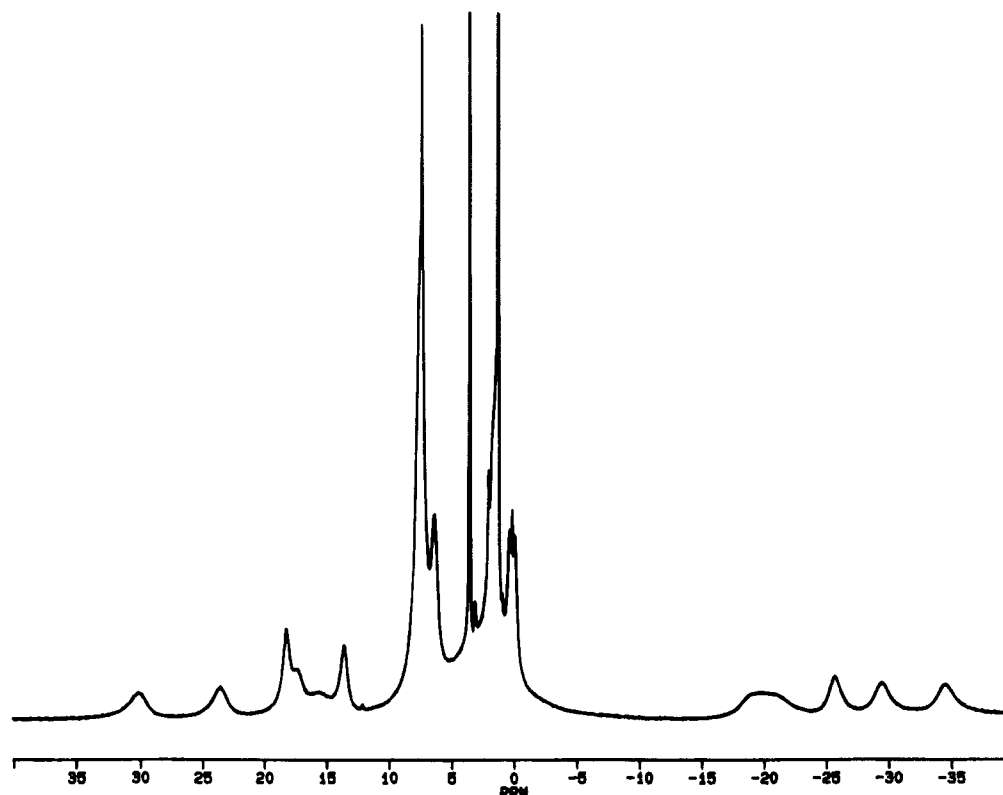


Figure 4.  $^1\text{H}$  NMR spectrum of complex **2** in  $\text{CDCl}_3$ .

Table 6. Paramagnetic Shifts (ppm) of 8-hqn Resonances of Unsymmetric Tricuclear Benzoate Complexes (and Assignments)

8-hqn	5-Cl-8-hqn	8-hqn-5,7- $d_2$	8-hqn	5-Cl-8-hqn	8-hqn-5,7- $d_2$
+29 (6 or 3)	+30	+29	-23 (5)		
+22 (6 or 3)	+23	+22	-25 (2 or 4)	-26	-26
+16 (6 or 3)	+18	+16	-29 (2 or 4)	-29	-29
+12 (6 or 3)	+13	+12	-33 (5)		
-18 (2 or 4)	-19	-18	-34 (2 or 4)	-34	-34
-19 (7)	-21				

<sup>a</sup> Numbers in parentheses indicate position of proton on hqn ring system.

were fit to a Hamiltonian equivalent to eq 3, resulting in two quite distinct coupling constants of ca.  $-38$  and  $-6$  K.

It is also of note that the symmetric  $\text{Cr}_3\text{O}$  species should undergo a small structural distortion as a result of symmetry lowering from a magnetic Jahn–Teller effect; the importance of such (which might result in measurable bond distance changes) is unknown.<sup>30</sup> The magnetic coupling in complexes **1** and **2** could be considered as the extreme example of the effect of symmetry lowering, albeit imposed by the ligands instead of a magnetic Jahn–Teller effect.

### NMR Spectroscopy

Recently, the utility of  $^1\text{H}$  and  $^2\text{H}$  NMR was demonstrated in the characterization of antiferromagnetically-coupled multinuclear chromium assemblies.<sup>14,22,31,32</sup> The reduction in  $\mu_{\text{eff}}/\text{Cr}$  and associated changes in  $T_1$  allow the paramagnetically shifted and broadened resonances to be observed. Independent

of the choice of solvent ( $\text{DMF-}d_7$ ,  $\text{DMSO-}d_6$ , or  $\text{CDCl}_3$ ), complexes **1–3** give rise to similar  $^1\text{H}$  NMR spectra with resonances ranging from  $+35$  to  $-35$  ppm. A representative  $^1\text{H}$  NMR spectrum of **2** is displayed in Figure 4.

Substitution of the benzoate ligands of complex **1** with  $\text{O}_2\text{-CC}_6\text{D}_5$  indicates that the benzoate proton resonances are limited to the range  $0$ – $8$  ppm, similar to those of the benzoate proton resonances of symmetric oxo-centered species.<sup>32</sup> The positions of these resonances are clearly shown in the  $^2\text{H}$  NMR spectrum of the  $\text{O}_2\text{CC}_6\text{D}_5$  derivative of complex **1** (Figure 5). The acetate methyl protons of complex **3** have unequivocally been assigned to overlapping resonances at ca.  $35$  ppm, using its  $\text{O}_2\text{CCD}_3$  derivative; the positions of these resonances are again similar to those of the symmetric species.<sup>32</sup> Thus, the remaining features in the upfield and downfield regions of the spectra of these complexes must arise from the hqn protons; this is consistent with a dominant  $\pi$ -delocalization mechanism giving rise to the paramagnetic shifts as expected for  $\text{Cr(III)}$  complexes.<sup>32</sup>

Attempts to assign the hqn resonances have been complicated by the low solubility of the complexes and their unsymmetric nature, which make all the hqn ligands inequivalent; however, use of selective substitution has been of some value (Table 6). At least 11 signals attributable to 8-hqn protons can be discerned; a maximum of 18 resonances would be expected for three inequivalent 8-hqn ligands. The  $^1\text{H}$  NMR spectrum of complex **2** (with 5-Cl-8-hqn) lacks two resonances at  $-23$  and  $-33$  ppm compared to the spectrum of complex **1**, indicating the missing resonances result from 5-position protons. The  $^1\text{H}$  NMR spectrum of an analogue of **1** with 8-hqn-5,7- $d_2$ <sup>18</sup> does not possess a resonance at  $-19$  ppm in addition to the resonances at  $-23$  and  $-33$  in the spectrum of **1**; similarly the  $^2\text{H}$  NMR spectrum of the 8-hqn-5,7- $d_2$  analogue displays signals at  $-20$ ,  $-23$ , and  $-33$  ppm. Hence, the resonance at  $-19$  ppm is assigned to a 7-position proton. As both the 5- and 7-position protons are shifted upfield and the magnitude of the shift of

(29) Goron, S. M.; Papaefthymiou, G. C.; Frankel, R. B.; Lippard, S. J. *J. Am. Chem. Soc.* **1987**, *109*, 4244–4255.

(30) Jayassoriya, U. A.; Cannon, R. D.; White, R. P.; Stride, J. A.; Grinter, R.; Kearley, G. J. *J. Chem. Phys.* **1993**, *98*, 9303.

(31) Belmore, K.; Madison, X. J.; Harton, A.; Vincent, J. B. *Spectrochim. Acta* **1994**, *50A*, 2365.

(32) Glass, M. M.; Belmore, K.; Vincent, J. B. *Polyhedron* **1993**, *12*, 133.

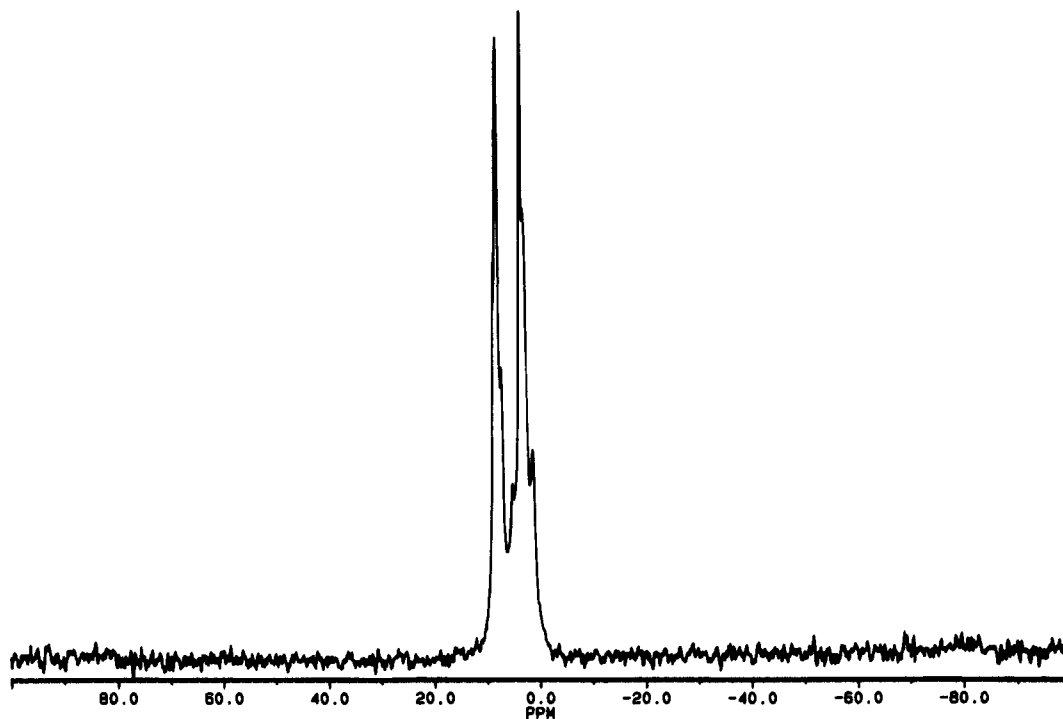


Figure 5.  $^2\text{H}$  NMR spectrum of  $\text{Cr}_3\text{O}(\text{O}_2\text{CC}_6\text{D}_5)_4(8\text{-hqn})_3$  in DMF.

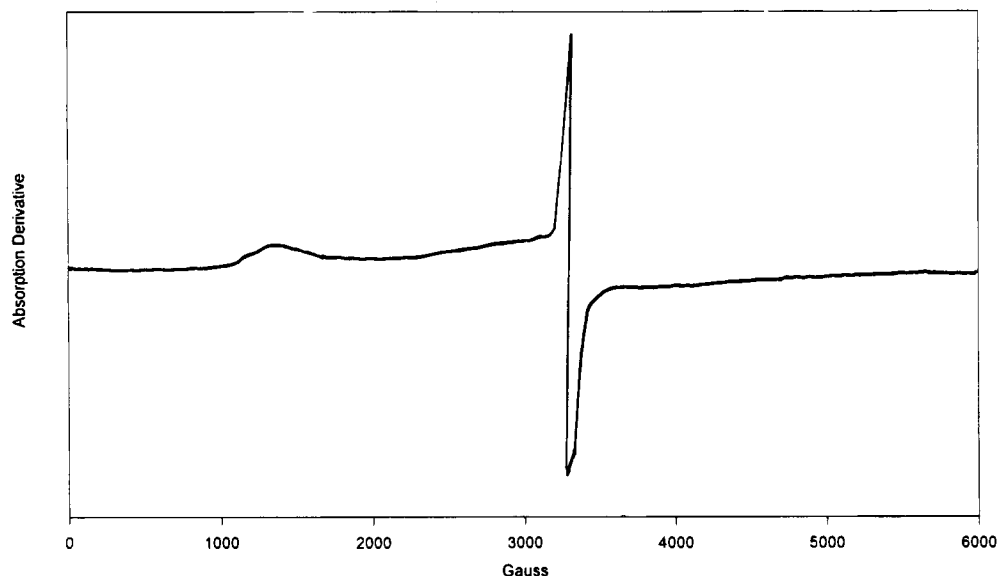


Figure 6. EPR spectrum of complex **1** in a MeOH glass at 11 K. Conditions: gain,  $5 \times 10^4$ ; scan time, 8 min; time constant, 0.5 s; modulation amplitude, 106; fieldset, 3000 G; scan range, 6000 G; power, 1 mW; frequency, 9.08 GHz.

Table 7. Mass (and Intensity) of Ions in Mass Spectra

ion	R = Ph, X = H	R = Me, X = H	R = Ph, X = Cl
$[\text{Cr}_3\text{O}(\text{O}_2\text{CR})_4(5\text{-X-8-hqn})_3]^+$	1088 (31.92) <sup>a</sup>	840 (33.57) <sup>a</sup>	1192 (33.48) <sup>b</sup>
$[\text{Cr}_3\text{O}(\text{O}_2\text{CR})_4(5\text{-X-8-hqn})_2]^+$	944 (42.86)	696 (56.72)	1014 (40.70)
$[\text{Cr}_3\text{O}(\text{O}_2\text{CR})_3(5\text{-X-8-hqn})_2]^+$	823 (8.45)		893 (6.66)
$[\text{Cr}_2(\text{O}_2\text{CR})_3(5\text{-X-8-hqn})_2]^+$	755 (17.90)	569 (13.35)	825 (6.82)

<sup>a</sup> Intensity relative to feature with mass 340 (100%) assigned to  $[\text{Cr}(8\text{-hqn})_2]^+$ . <sup>b</sup> Intensity relative to feature with mass 408 (100%), assigned to  $[\text{Cr}(5\text{-Cl-8-hqn})_2]^+$ .

the 7-position is not attenuated compared to that of the 5-position proton, a  $\pi$  delocalization is clearly in operation. Thus, because of the alternating sense of the shift of protons about a ring for a  $\pi$ -delocalization mechanism, the 6-position proton resonance is expected to be shifted downfield. For the protons of the pyridine ring of the hqn ligand, the 2- and 4-position proton

resonances are expected to be shifted upfield and the 3-position proton resonance is expected to shift downfield, on the basis of the spectra of symmetric trinuclear complexes with monodentate pyridine ligands.<sup>32</sup>

#### EPR

The X-band EPR spectrum of complex **1** in  $1.25\text{CH}_2\text{Cl}_2$  in a methanol glass at 11 K is shown in Figure 6. The spectrum possesses two dominant features with  $g$  values of approximately 4 and 2. Thus, the spectrum is consistent with the results of the variable magnetic susceptibility studies which indicated that the complex possessed an  $S = 3/2$  ground state with a low-lying  $S = 1/2$  first excited (only  $|3J|$  above the ground state).

(33) Vincent, J. B. *Inorg. Chem.* **1994**, *33*, 5604.

(34) van den Bergen, A.; Colton, R.; Percy, M.; West, B. O. *Inorg. Chem.* **1993**, *32*, 3408.

### Mass Spectra

Fast atom bombardment mass spectrometry was recently shown to be a valuable technique in the characterization of cationic oxo-bridged multinuclear Cr assemblies<sup>14,22</sup> and heteronuclear Cr/Fe assemblies.<sup>33</sup> However, for these neutral complexes, FAB has only been of limited utility, while electron impact (EI) mass spectrometry of these complexes reveals a distinctive set of ions with mass corresponding to the parent ion and fragments of the parent ion derived by loss of carboxylate or bidentate ligand (Table 7). Similar bidentate ligand and carboxylate loss has been observed in FAB mass spectrometric studies of cationic tetranuclear Cr-oxo species.<sup>22</sup> Monodentate terminal ligand loss but not carboxylate loss has

been observed for cationic Cr-oxo complexes in electrospray mass spectrometric studies; carboxylate loss required collision activation.<sup>34</sup>

**Acknowledgment** is made to the donors of the Petroleum Research Fund, administered by the American Chemical Society, and the American Heart Association (J.B.V.) for support of this research.

**Supporting Information Available:** Tables of crystallographic experimental details, thermal parameters, and bond distances and angles for **1**, a figure with the complete labeling scheme for **1**, and figures of  $\chi$  vs  $T$  for **1** and **3** (18 pages). Ordering information is given on any current masthead page.

IC9414839